Osteology and Cranial Musculature of *Caiman latirostris* (Crocodylia: Alligatoridae)

Paula Bona[1,2]* and Julia Brenda Desojo[2,3]

[1]*División Paleontología Vertebrados, Facultad de Ciencias Naturales y Museo, Paseo del Bosque s/n, 1900, La Plata, Buenos Aires, Argentina*
[2]*CONICET, Consejo Nacional de Investigaciones Científicas y Técnicas, Argentina*
[3]*Sección Paleontología de Vertebrados, Museo Argentino de Ciencias Naturales "Bernardino Rivadavia," Av. Angel Gallardo 470 C1405DRJ, Capital Federal, Argentina*

ABSTRACT *Caiman latirostris* Daudin is one of the extant species of Caimaninae alligatorids characterized taxonomically only by external morphological features. In the present contribution, we describe the cranial osteology and myology of this species and its morphological variation. Several skull dissections and comparisons with other caimans were made. Although jaw muscles of living crocodiles show the same general "Bauplan" and alligatorids seem to have a similar cranial musculature pattern, we describe some morphological variations (e.g., in *C. latirostris* the superficial portion of the *M. adductor mandibulae externus* did not reach the postorbital; the *M. adductor mandibulae internus pars pterygoideus dorsalis* did not reach the pterygoid and lacrimal and contrary to the case of *C. crocodilus* the *M. adductor mandibulae internus pars pterygoideus ventralis* attaches to the posterodorsal surface of the pterygoid and the pterygoid aponeurosis, without contacting the dorsal and ventral surface of the pterygoid margin; the *M. intermandibularis* is attached to the anterior half of the splenial and posteriorly inserts medially by a medial raphe that serves as attachment zone for *M. constrictor colli*, and the *M. constrictor colli profundus* presents a medial notch in its anterior margin). In addition, the skull of *C. latirostris* differs from that of other caimans and possesses several characters that are potential diagnostic features of this species (e.g., outline of glenoid cavity in dorsal view, extension of the rostral ridges, and occlusion of the first dentary tooth). Nevertheless, these characters should be analyzed within the phylogenetic context of the Caimaninae to evaluate its evolutionary implications for the history of the group. J. Morphol. 000:000–000, 2011.

KEY WORDS: Crocodylia; Alligatoridae; Caimaninae; *Caiman latirostris*; cranial osteology; cranial myology

INTRODUCTION

Crocodiles and birds represent the two extant archosaurian groups and their cranial anatomy has attracted the interest of many researchers since the 19th century (Iordansky, 1973). Although many studies describe the cranial morphology of extant alligatorids (e.g., Brochu 1999; Rowe et al., 1999) or caimans [e.g., *C. crocodylus* (Daudin); Iordansky, 1973; Schumacher, 1973; Van Drongelen and Dullemeijer, 1982; Cleuren and De Vree, 2000], our knowledge of the morphological variation among different living species is limited (Carvalho, 1951; Diefenbach, 1979), and several of these taxa are not properly defined by osteological features. The taxonomic diversity of the fossil record of alligatorids is wider than the extant, and fossil species are defined by cranial and jaw osteological characters. In contrast, living taxa are currently defined by external morphological characters. This makes it difficult to understand the evolutionary history of the crown group "Caiman" (*sensu* Brochu, 1999). The genus *Caiman* Spix currently contains three extant species, *C. latirostris* (Daudin), *C. crocodylus*, and *C. yacare* (Daudin) but the taxon might be paraphyletic (Fig. 1; Norell, 1988; Brochu, 1999, 2003). Although the cranial musculature, in particular the jaw muscles, has been analyzed in *C. crocodylus* (Schumacher, 1973; Van Drongelen and Dullemeijer, 1982), the musculature of the other South American species, as well as the morphological variability of the cranial musculature and its attachment sites on the skeleton are poorly known. This study aims to analyze the cranial morphology of the most extreme broad-snouted form among the *Caiman* species, *C. latirostris*, to describe the cranial osteology and myology of this species and its osteological cranial variation. Complementarily, a quantitative comparison between *C. latirostris* and *C. yacare* is provided.

*Correspondence to: Paula Bona, Departamento de Paleontología Vertebrados, Museo de La Plata, Paseo del Bosque s/n, 1900, Argentina. E-mail: pbona@fcnym.unlp.edu.ar

Received 10 November 2009; Revised 29 May 2010;
Accepted 25 June 2010

Published online in
Wiley Online Library (wileyonlinelibrary.com)
DOI: 10.1002/jmor.10894

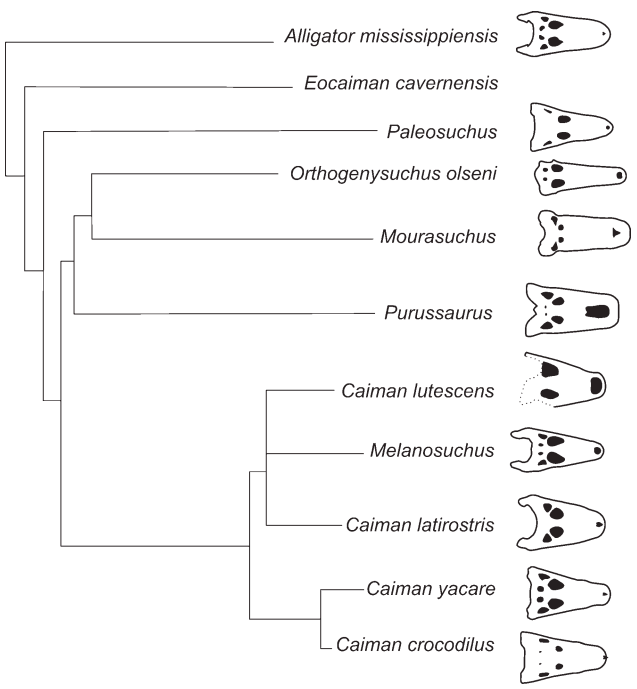

Fig. 1. Cladogram showing the phylogenetic position of *Caiman latirostris* (modified from Brochu, 2003).

MATERIALS AND METHODS

For the osteological analysis, 120 specimens of *C. latirostris* and *C. yacare* at different ontogenetic stages were analyzed: 100 specimens of *C. yacare* and 20 of *C. latirostris* were housed at the herpetological collections of Museo Argentino de Ciencias Naturales (MACN) "Bernardino Rivadavia" and Museo de La Plata. Quantitative analysis was carried out on the skull of 37 specimens of different sizes of both species. The sample size for each species was chosen according to the availability of ontogenetic series with complete skulls in the collections. The following skull measurements were taken using a digital caliper (0.01 mm): total cranial length (measured dorsally along the sagital axis from the tip of the premaxilla to the posterior margin of the skull table); snout length (measured dorsally along the sagital axis from the tip of the premaxilla to the anterior margin of the orbits); anterior snout width (measured dorsally and perpendicularly to the sagital at the premaxillary–maxillary suture); posterior snout width (measured dorsally and perpendicularly to the sagital at the anterior margin of the orbits); and interorbital minimum width. The relationship between these traits and the overall size, in the postnatal ontogeny in both species of *Caiman*, was analyzed using linear regression. For this purpose, the data were $\log_{10}$ transformed and bivariate equations were calculated. The slope (b), intercept ($\log a$), and confidence intervals were calculated using ordinary least squares regression (OLS) and standardized major axis (Legendre and Legendre, 1998). Because of the high correlation between the skull variables analyzed, similar results were obtained with two methods; here we report OLS results.

For the myological cranial analysis, two subadult specimens of *C. latirostris* and one subadult specimen of *C. yacare* were analyzed. This material was provided by the staff of "El Cachape" and "Proyecto Yacaré" in the provinces of Chaco and Santa Fe of Argentina, respectively. The specimens were dissected at the Laboratory of Vertebrate Anatomy at the Facultad de Ciencias Naturales, Universidad Nacional de La Plata (School of Natural Sciences) and also in the Herpetology Department of Museo de La Plata, Argentina. All specimens were obtained fresh, frozen, or fixed in 10% neutral buffered formalin and sectioned using a scalpel. All dissections were documented by digital photography. Attachment areas were examined on the osteological material. The myological study proceeded from the most superficial muscles to the deepest ones, removing the jugal and quadratojugal bones, the postorbital processes, and finally part of the maxilla.

We follow Romer (1956) for osteological nomenclature and Sedlmayr (2002) for the nomenclature of nerves and blood vessels. The main cranial muscular groups were identified based on the main muscle innervations (e.g., trigeminal, facial, glossopharyngeal, hypoglossal nerves) following Iordansky (2000) and Schumacher (1973). In the case of the adductor chamber, we followed Holliday and Witmer (2007) (Tables 1 and 2). The relative position of the ophthalmic, maxillary, and mandibular divisions of the trigeminal nerve distinguish different groups of jaw muscles, namely *M. adductor mandibulae internus* (MAMI), *M. adductor mandibulae externus* (MAME), *M. adductor mandibulae posterior* (MAMP), and *M. constrictor internus dorsalis* (MCID). In the case of the trigeminal muscles, this paper focuses primarily on the adductor musculature proper (i.e., *M. adductor mandibulae*) and does not include the MCID.

RESULTS

Cranial Osteology

In dorsal view, the skull of *C. latirostris* has a triangular outline with the lateral margins converging anteriorly. In other caimans, the lateral margin of the rostral area is wavy. In this view, the premaxillary–maxillary curvature is practically absent (Fig. 2A,B). The lateral margins of the skull in the postorbital region are straight or slightly concave, diverging from one another posteriorly. In all specimens, the lateral processes of the squamosal are short and posterolaterally oriented. The posterior margin of the skull table is straight and perpendicular to the sagittal plane (posterior margins of supraoccipital and two-thirds of squamosal, approximately). In adults, the supratemporal fenestra is small, irregular, and anteroposteriorly elongated. In dorsal view, the anterior opening of the temporal canal in the supratemporal fenestra is vertically oriented and covered by the squamosal. The infratemporal fenestra is triangular in outline and its anteroposterior length is half of the orbit (Fig. 2A). It is limited ventroposteriorly by the quadratojugal bone, which extends along the posterior margin but does not reach the posterodorsal corner of the fenestra. In the orbital area, the interorbital isthmus is pronounced. The interorbital surface is concave, and the medial margin of the orbit describes a crest, which projects anteriorly across the prefrontal bone, lacrimal bone, and maxillae, almost reaching the lateral margin of the rostral area (Fig. 2A). In front of the orbit, this crest (paired) extends medially, forming a transversal "u" like structure. In occipital view (Fig. 2D), the posterodorsal margin of the skull is slightly concave at the supraoccipital, horizontal at the medial portion of the squamosal, and ventrally projected at the lateral part of the squamosal bone. The paroccipital projections are laterally short and horizontally oriented. The supraoccipital

TABLE 1. Trigeminal muscles (Iordansky, 2000) in C. latirostris

		Origin	Insertion
M. adductor mandibulae externus (Holliday and Witmer, 2007)		Ventral surface of the quadrate and quadratojugal (its superficial pars contacts the postorbital)	Aponeurosis coronar, transiliens cartilage, and dorsal border of surangular
M. adductor mandibulae posterior (Holliday and Witmer, 2007)		Ventral surface of the quadrate	Medial border of the articular, medial margin of the angular, medial area of the surangular, and caudal portion of the transiliens cartilage
M. aductor mandibulae internus (Holliday and Witmer, 2007)	*M. pseudotemporalis* (= *M. Pseudotemporalis superficialis and profundus sensu* Holliday and Witmer, 2007)	Laterosphenoid	Dorsal surface of the transiliens cartilage
	M. intramandibularis (sensu Iordansky, 1964)	Transiliens cartilage (intramandibular aponeurosis, Iordansky 2000)	Medial surface of the dentary, splenial, angular and Meckelian cartilage
	M. pterygoideus dorsalis (Holliday and Witmer 2007)	Medial and anterior margin of the suborbital fenestra, maxilla, prefrontal and orbitonasal and interorbital cartilages	Anterolaterally and posteromedially to the mandibular tendon
	M. pterygoideus ventralis (Holliday and Witmer 2007)	Dorsoposterior surface of pterygoid and pterygoidal aponeurosis (*sensu* Iordansky, 2000)	Posterior and medial border of the retroarticular process
M. intermandibularis (Holliday and Witmer, 2007)		Anterior half of each splenial	The opposite splenial bone, anteriorly and in a medial raphe, posteriorly

Origins (dorsal attachments), insertions (ventral attachments),and terms followed in this study.

TABLE 2. Facial, glossopharyngeal, hypoglossal, and hypobranchial longitudinal muscles in C. latirostris

		Origin	Insertion
Facial muscles (Iordansky, 2000)	*M. constrictor colli*	An aponeurosis of *M. pterygoideus ventralis* and laterally to the first two cervical vertebrae (*sensu* Schumacher 1973)	Medial tendinous raphe and posteroventral tendinous zone of the hyoids
	M. depressor mandibulae	Posterodorsal margin of supraoccipital, squamosal, and posterodorsal surface of quadrate	Dorsal surface of the retroarticular process
Glossopharyngeal muscles (Schumacher, 1973)	*M. branchiomandibularis visceralis*	Lateral margin of hyoids	Anteroventral surface of angular
Hypoglossal muscles (Schumascher, 1973)	*M. branchiomandibularis spinalis*	Basal end of the *Cornu branchiale I* of hyoids	Medial and dorsal surface of splenial
	M. hyoglossus	Dorsolateral, posterior and ventral border of the posterior corner of the hyoid	Connective raphe at the base of the tongue (its fibers are anteriorly interdigitated forming the tongue)
	M. genioglossus	Mandibular symphysis	Anterior border of the hyoid (its fibers extends posterolaterally surrounding the *M. hyoglossus*)
	M. coracohyoideus	Coracoid	Posterior process of the hyoid
Hypobranchial longitudinal muscles (Schumacher, 1973)	*M. episternobranchiotendineus*	Sternum	Medial surface and posterodorsal margin of the splenial
	M. episternobranchialis	Sternum	Ventrolateral area of the hyoid body, medially to the *cornu branchialis I*

Origins (dorsal attachments), insertions (ventral attachments),and terms followed in this study.

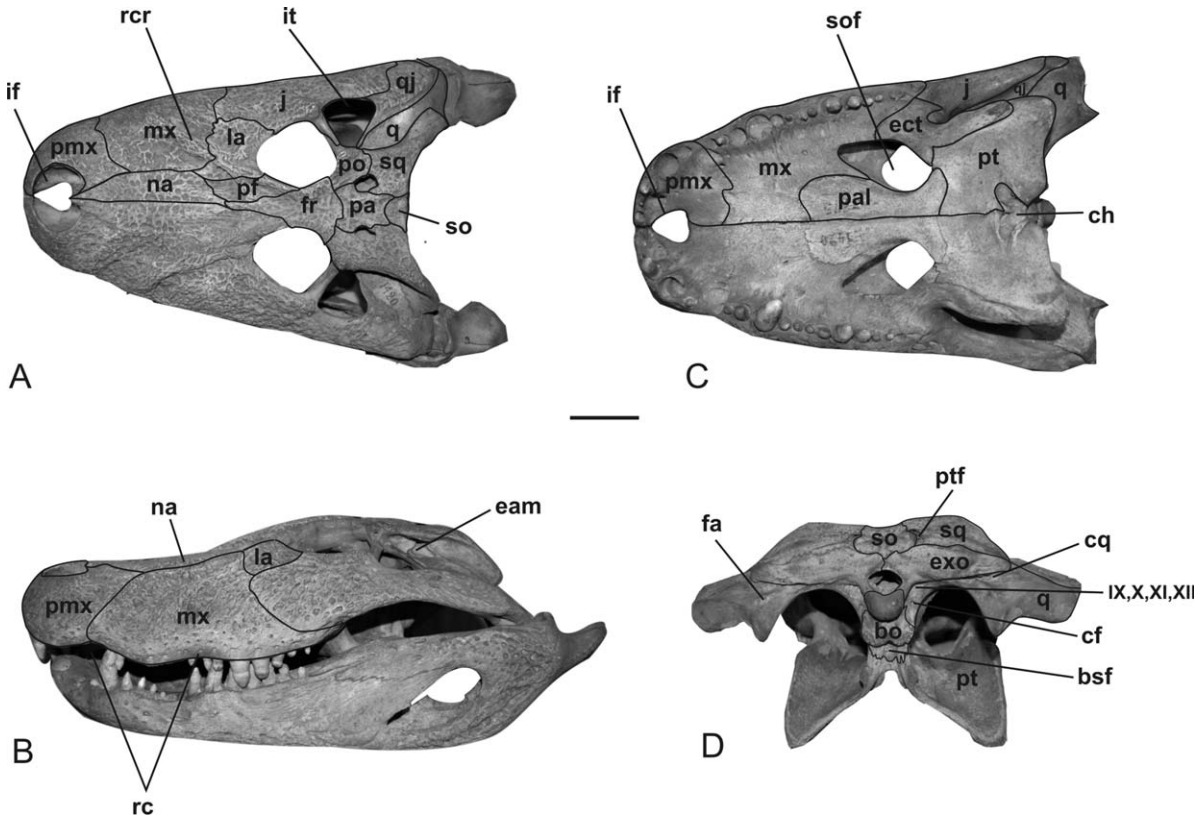

Fig. 2. Skull of *C. latirostris* (MACN V 1420): **A**, dorsal; **B**, lateral; **C**, palatal; **D**, occipital views. Scale bar equals 5 cm. bo, basioccipital; bsf, basisphenoid; ch, choanae; cf, carotid foramen; cq, cranioquadrate canal; eam, external auditory meatus; ect, ectopterigoid; exo, exoccipital; fa, foramen aërum; fr, frontal; if, incisive foramen; it, infratemporal fenestra; j, jugal; la, lacrimal; mx, maxilla; na, nasal; pa, parietal; pal, palatine; pf, prefrontal; pmx, premaxilla; po, postorbital; pt, pterigoid; ptf, postemporal fenestra; q, quadrate; qj, quadratojugal, rc, rostral curvatures; rcr, rostral crest; sq, squamosal; so, supraoccipital; sof, suborbital fenestra; f IX, f X, f XI, f XII, 9–12° cranial nerve foramens.

bone is low and wide, pentagonal, and forms the ventromedial margin of the post-temporal fenestra, which is much reduced in this species. The foramen magnum is delimited mostly by the exoccipital bones and by the basioccipital at the medial ventral portion. The exoccipitals are sutured at the midline and project ventrally, lateral to the basioccipital tubera (as in many Caimaninae; Fig. 2D). In occipital view, the subtemporal fossa is more depressed than in other *Caiman* species (e.g., *C. yacare*) and is limited mainly by the quadrate bone dorsally and the pterygoid ventrally.

In palatal view, the palatine isthmus is present and slightly displaced to the posterior sector of the medial margin of the suborbital fenestrae (Fig. 2C). The suborbital fenestrae are limited by the palatine medially and posteriorly, the pterygoid posteriorly, the ectopterygoid posterolaterally, and the maxilla anteriorly and anterolaterally. The external surfaces of the dermal bones are sculptured and covered with ridges and cells as in other species of *Caiman*. This sculpturing is pronounced on the skull and least developed on the lower jaw, where it is strongly marked on the lateral surfaces of the angular and surangular bones, posterior to the external mandibular fenestra (Fig. 3A). The number of mandibular teeth ranges from 17 to 19. The length of the mandibular symphysis is variable and extends to the alveoli fifth, fifth/sixth. As in other caimans, the lateral margin of the dentary bone in lateral view presents two stout flexures, the first between alveoli first and fourth and the second between fifth and tenth alveoli. The external mandibular fenestra is delimited by the dentary anteriorly and anteroventrally (in small proportion), the angular posteroventrally, and the surangular posterodorsally. The extension of the dentary along the ventral margin of the external mandibular fenestra is variable in *Caiman* species and in one specimen of *C. latirostris* (MACN 30566) the dentary did not delimit the fenestra. The internal mandibular fenestra is delimited by the angular ventrally, the articular posteriorly and posteroventrally, and the coronoid anteriorly and anteroventrally (Fig. 3B). The ovate foramen intermandibularis caudalis is horizontally oriented and delimited by the angular posteriorly and the splenial anteriorly.

Basioccipital bone. In occipital view (Fig. 2D), the basioccipital bone is wider and hexagonal in

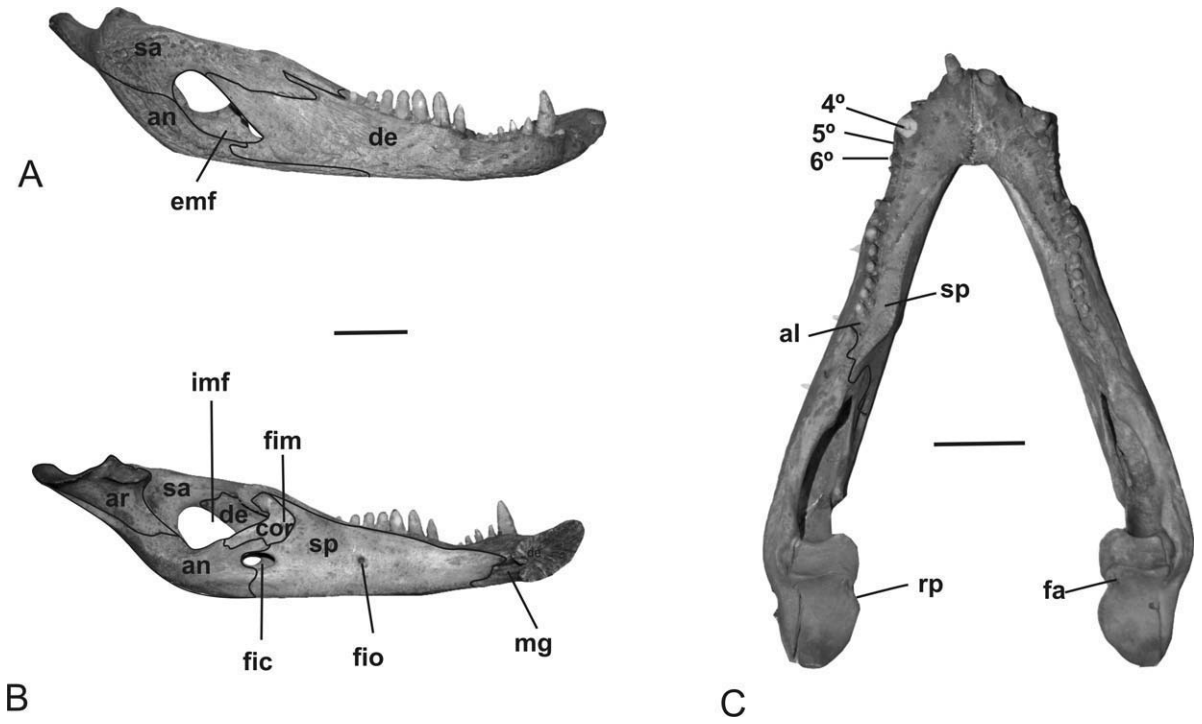

Fig. 3. Lower jaw of *C. latirostris* (MACN V 1420): **A**, lateral; **B**, medial; **C**, dorsal views. Scale bar equals 5 cm. al, alveolous (4°, 5°, 6°); an, angular; ar, articular; cor, coronoid; de, dentary; emf, external mandibular fenestra; fa, foramen aërum; fic, foramen intermandibularis caudalis; fim, foramen intermandibularis medius; fio, foramen intermandibularis oralis; imf, internal mandibular fenestra; mg, meckelian groove; rp, retroarticular process; sa, surangular; sp, splenial.

shape. It contacts the basisphenoid ventrally and the exoccipitals laterally and dorsally. Together with the basisphenoid, it delimits the single medial opening and the paired lateral openings of the Eustachian tubes ventrally. It forms the occipital condyle and the medioventral margin of the foramen magnum dorsally and extends anteriorly forming the posterior floor of the braincase.

Exoccipital bone. In occipital view, each exoccipital extends horizontally forming a short paroccipital projection (Fig. 2D) and contacts the squamosal dorsolaterally, the supraoccipital dorsomedially, the quadrate ventrolaterally, and the basioccipital ventromedially. In lateral view, each exoccipital contacts the quadrate anterodorsally and the basisphenoid anteroventrally. The exoccipitals also contact each other on the midline delimiting the ventrolateral, lateral, and dorsal margins of the foramen magnum. The following foramina open lateral to the foramen magnum: 1) Openings for cranial nerves IX, X, XI, and XII. In *C. latirostris* these are three horizontally aligned openings. From medial to lateral, they correspond to the opening for the XII2 branch which innervates part of the neck muscles, a middle opening for the XII1 branch which innervates the hyoglossus, sternohyoideus, and sternothyroideus muscles (see below), and the most lateral opening for nerves IX, X, and XI. This last foramen is the largest, and in all specimens of this species it presents an internal bony septum that separates the opening for the IX nerve (medial) from the opening for the nerves X and XI (lateral). 2) Carotid foramen. This is most ventral in position, located near the lateral margin of the exoccipital. The internal carotid arteries pass through this foramen. 3) Cranioquadrate canal. This canal extends between the paroccipital process and the quadrate (Fig. 2D) from the middle ear cavity to the occipital surface, where it opens on the medioventral margin of the paroccipital process. It corresponds to the passage for the hyomandibular branch of the facial nerve (VII; mainly the VII3 branch that innervates the *M. depressor mandibulae* and another branch that innervates the *chorda tympani*), the orbitotemporal artery, and the lateral cephalic vein (Iordansky, 1973; temporoorbital artery and vein *sensu* Sedlmayr, 2002).

Supraoccipital bone. The supraoccipital has a triangular outline in occipital view (Fig. 2D). It contacts the squamosal laterally and the exoccipital ventrally, together delimiting the post-temporal fenestrae. These fenestrae provide the passage for vessels that stem from the orbitotemporal artery and vein (Sedlmayr, 2002). As in other Caimaninae, the supraoccipital bone extends on the posterior surface of the skull table and in dorsal view it contacts the parietal anterolaterally and the squamosal posterolaterally. The dorsal surface is

slightly concave with a poorly pronounced median crest. This crest is more pronounced in adult specimens; this ontogenetic variation was also observed in *C. yacare*.

Basisphenoid. The basisphenoid forms the anterior floor of the braincase and extends anteriorly into the interorbital space forming the sphenoidal rostrum. The basisphenoid is exposed in occipital view, reaching the basioccipital bone dorsally and pterygoid ventrolaterally. In posterolateral view, it contacts the quadrate anterodorsally, the pterygoid anteroventrally, the exoccipital bone posterodorsally, and the basioccipital bone posteroventrally.

Laterosphenoid. Each laterosphenoid forms the anterolateral wall of the braincase and extends dorsally forming the anteroventral area of the medial wall of the supratemporal fossa. In lateral view, it contacts the quadrate, pterygoid and prootic bone posteriorly, the pterygoid ventrally, the basisphenoid anteroventrally, and the frontal and postorbital dorsolaterally. Together with the prootic bone it delimits the anterior part of the trigeminal opening (Fig. 4A,B). Laterally it presents a laterosphenoid bridge, which in *C. latirostris* is a descending process of the laterosphenoid that ventrally forms a suture with the pterygoid, delimiting a passage for the ophthalmic trigeminal branch (V1; Fig. 4A). It also provides an attachment surface for the *M. pseudotemporalis profundus* (sensu Holliday and Witmer, 2007; Walker, 1990). The constitution and morphology of this bridge is variable in crocodiles (Brochu, 1999: 64; figure 52) and even in *Caiman* (e.g., *C. latirostris*, *C. yacare*). In *C. latirostris*, it is wide and broadly sutured to the pterygoid (see below). As in other *Caiman* species, the laterosphenoid also forms a broad caudal bridge for the passage of the supraorbital nerve (Holliday and Witmer, 2009) that articulates with the quadrate.

Prootic bone. As in other living crocodylians, the prootic bone is not broadly exposed on the lateral braincase wall and forms the posterior margin of the trigeminal foramen.

Squamosal bone. Together with the postorbital, the squamosal delimits the supratemporal fenestra ventrally. It contacts the postorbital and parietal dorsally, supraoccipital and exoccipital posteroventrally, and postorbital and quadrate anteroventrally. In occipital view, a subhorizontal ridge is present that divides the surface of the squamosal into two equivalent areas, the dorsalmost portion of which is part of the attachment site of the *M. depressor mandibulae* (Fig. 2D). In lateral view, the squamosal forms the roof of the tympanic cavity.

Parietal bone. Both parietal bones are fused at the midline and form the anteromedial margin of the supratemporal fenestra and the medial wall of the supratemporal fossa. The parietal bone contacts the frontal bone anteriorly, the postorbital and squamosal bones laterally, and the supraoccipital bone posteriorly. Together with the supraoccipital, the parietal forms a shallow depression with two smooth lateral ridges (Fig. 2A). These ridges extend from the medial edge of the supratemporal fenestra to the posterior margin of the skull table.

Postorbital bone. As in other crocodiles, this bone forms the anterior part of the supratemporal bridge at the anterolateral sector of the skull table and also the anterolateral wall and margin of the supratemporal fossa and fenestra, respectively. It delimits the orbit posteriorly, by means of a descending process that is sutured to the ascending process of the jugal bone. Its contacts are with the jugal ventrally, the squamosal and quadrate posteriorly, the laterosphenoid medially, and the frontal anteriorly.

Frontal bone. Both frontal bones are fused at the midline forming a single bone that delimits part of the orbit medially and projects anteriorly between the prefrontal bones. This projection reaches the nasal bones in some specimens. It also presents an interorbital isthmus and a concave dorsal surface that together with the prefrontal determines the medial orbital crest. The ventral surface has a medial groove for the articulation of the interorbital septum. The frontal contacts the parietal dorsally and the postorbital posteriorly (Fig. 2A).

Prefrontal bone. Each prefrontal bone is located anteromedial to the orbit forming the anterior part of the medial margin (crest) of the orbit. The prefrontal contacts the frontal medially, the nasal anteriorly, and the lacrimal laterally. It has a ventromedial descending process, perpendicular to the sagittal plane for the orbitonasal cartilaginous septum. Ventrally, this process contacts primarily with the palatine and the pterygoid.

Lacrimal bone. The lacrimal bone forms the anterior margin of the orbit. The anterior margin of the lacrimal (lacrimal–maxilla suture) possesses a medial projection (Fig. 2A) that extends anteriorly between the nasal and maxilla. The lacrimal gland is enclosed within the lacrimal bone and is oriented longitudinally parallel to the sagittal plane and opens posteriorly on the anterior margin of the orbit. In dorsal view, the lacrimal contacts the prefrontal and nasal medially, the jugal laterally, and the maxilla anteriorly.

Nasal bone. Each nasal is an elongate bone that extends anteroposteriorly in the medial sector of the snout reaching the external narial fenestrae in some specimens (Fig. 2A). The nasal is a narrow bone with lateral margins tapering anteriorly; in some specimens these lateral margins extend into the narial space and form a "heart-like" outline for the narial opening. Both nasals form the roof of the nasopalatine duct and posteriorly overlap the frontals.

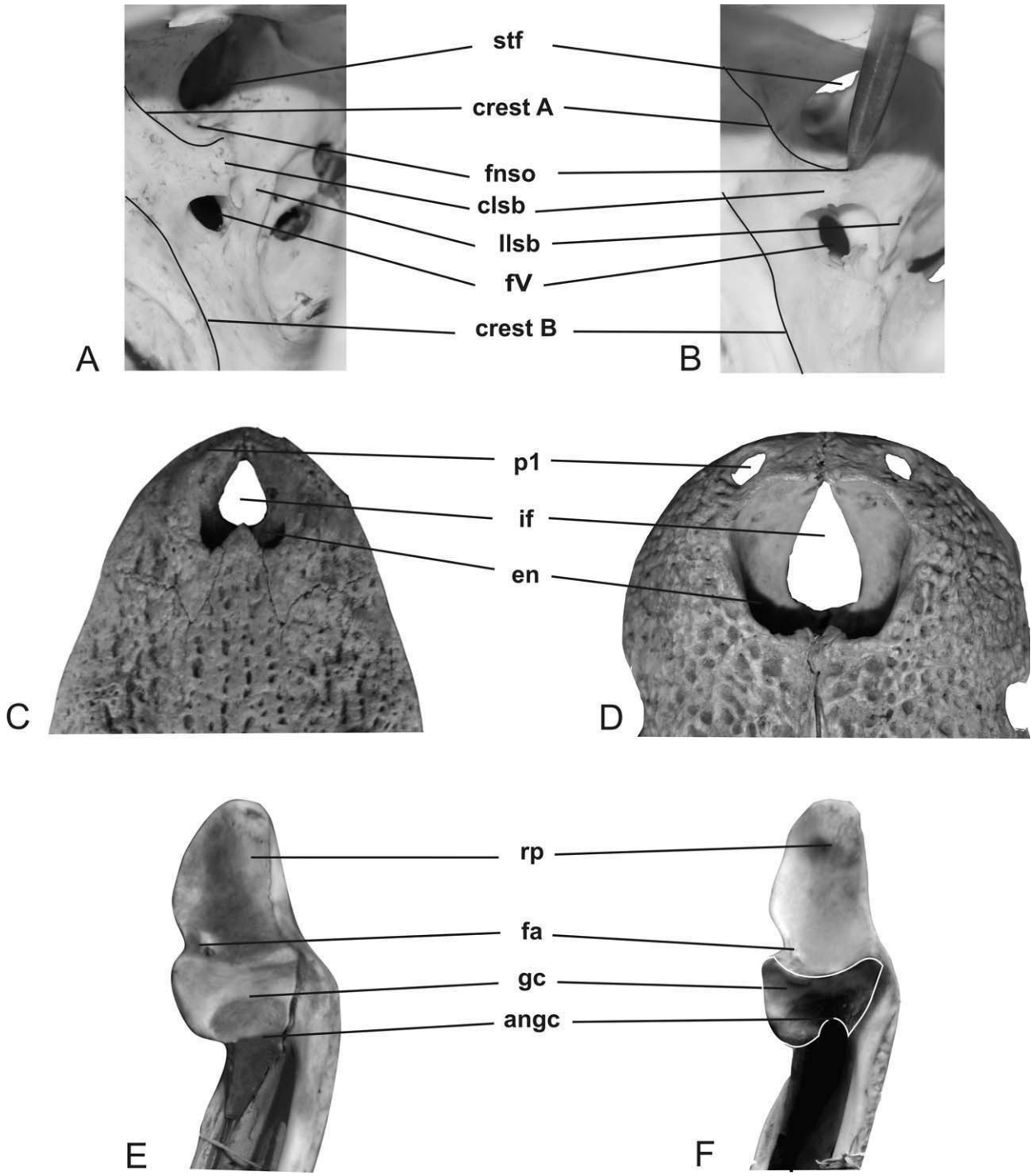

Fig. 4. Detail of osteological cranial characters. **A** and **B**, Lateral view of the ventral surface of the quadrate: A, *C. latirostris*; B, *C. yacare*. **C** and **D**, Dorsal view of the premaxilla: C, *C. latirostris*; D, *C. yacare*. **E** and **F**, Dorsal view of the retroarticular process: E, *C. latirostris*; F, *C. yacare*. angc, anterior notch of the glenoid cavity; clsb, caudal laterosphenoid bridge; en, external nares; fa, foramen aërum; fcno, supraorbital foramen; fV, trigeminal foramen; gc, glenoid cavity, if, incisive foramen; llsb, lateral laterosphenoid bridge; p1, piercing of the first lower teeth; rp, retroarticular process; stf, supratemporal fossa.

Vomer. Both vomers are slender and meet at the midline forming the sulcus for the internasal cartilaginous septum. The vomer extends posteriorly near the descending process of the prefrontal bone. In ventral view, the vomers are covered by the secondary palate.

Quadrate. The quadrate extends posterolaterally in the posterior portion of the skull and it is

sutured to surrounding bones, with the exception of the otic sinovial articulation (see Holliday and Witmer, 2008). The quadrate contacts the exoccipital and squamosal dorsally, the postorbital and quadratojugal anterolaterally, and the laterosphenoid, prootic, pterygoid, basisphenoid, and exoccipital ventromedially. Posteroventrally, the quadrate forms the mandibular condyle. In occipital view, a foramen aërum is present (see Brochu, 1999: 36, figures 24C and D). In lateral view, the quadrate has a medial concave zone that represents the lateral floor of the middle ear cavity and whose semicircular lateral margin supports the tympanic membrane. Medially, the quadrate forms the ventral, dorsal, and anterior margins of the external auditory meatus, which is heart shaped. In ventral view, two crests are present, A and B *sensu* Iordansky (1964), for the attachment of the *M. adductor mandibulae externus* and M. adductor mandibulae posterior. Crest A runs parallel to the quadrate–quadratojugal suture and the medial margin of the upper temporal fossa, while crest B is vertically oriented posterior to the foramen for nerve V and extends along the pterygoid. In *C. latirostris* these crests are not prominent and crest B tapers ventrally toward the posteroventral border of the quadrate. The ventral surface of the quadrate projects anterodorsally to form the ventral portion of the posterior wall of the supratemporal fenestra. A small foramen is present in this area, dorsal to crest A, for the passage of the supraorbital nerve (sensu Holliday and Witmer, 2009; Fig. 4A,B) and probably the middle cerebral vein.

Quadratojugal bone. The quadratojugal bone forms the posterior margin of the infratemporal fenestra, reaching its dorsal corner. In lateral view, the quadratojugal forms the infratemporal arch together with the jugal and contacts the jugal anteriorly, the postorbital dorsally, and the quadrate posteriorly.

Jugal bone. The jugal bone is an elongated bone that delimits the ventral border of the orbit and the infratemporal fenestra. In dorsal view, the jugal contacts the lacrimal medially, the maxilla anteriorly, and the quadratojugal posteriorly. Its lateral margin is straight, but in lateral view, its ventral margin is concave and projects dorsally via an ascending process, which together with the postorbital delimits the orbit (Fig. 2A,B). As in other crocodiles, its dorsal margin descends abruptly in the postorbital region. In ventral view, the jugal is positioned lateral to the maxilla, taking the form of an anterior process that projects at least to the level of the last two alveoli. In this view, the jugal contacts the maxilla and ectopterygoid medially.

Maxilla. The maxilla contacts the jugal, prefrontal, and lacrimal posteriorly, the nasal laterally, and the premaxilla posteriorly. Its dorsal surface bears a crest that extends toward the anterior margin of the orbit. This crest extends anterolaterally but does not reach the lateral border of the maxilla. In its anterior part and in lateral view, the ventral margin of this bone is convex with two slight curvatures. The maxilla possesses 12 or 13 alveoli. In palatal view, the maxilla contacts the premaxilla anteriorly, the jugal posterolaterally, the ectopterygoid posteriorly, and the palatine posteromedially. Together with the premaxilla and palatine, the maxilla forms the anterior floor of the nasopalatine duct. The openings of the postvestibular recess, anteromedially, and the caviconchal recess, posterolaterally (Witmer, 1995), are present on the medial surface of the maxilla.

Premaxilla. The premaxilla forms the anterolateral margin of the snout, contacting the maxilla posteriorly. The premaxilla projects dorsomedially and delimits the external naris forming a posterolateral ridge. In some specimens the premaxillae contact each other dorsomedially, excluding the nasals from the posterior margins of the external nares. In palatal view, the premaxilla delimits the incisive foramen, which in *C. latirostris* is heart or teardrop shaped. The anterior ventral surface of each premaxilla has a cavity that receives the first mandibular tooth. In some specimens of *C. latirostris*, this tooth pierces the palatal surface of premaxilla (but never its dorsal anterior surface, as in *C. yacare* or *C. crocodylus*; Fig. 4C,D).

Palatine bone. In palatal view, the palatine bones contact one another at the midline and delimit the suborbital fenestra medially. Anterior to the fenestra, the palatines expand mediolaterally and possess a rounded outline that is wider anteriorly.

Pterygoid. The pterygoids meet each other along the midline both dorsally and ventrally, forming the medial wall and roof of the middle part, and all of the posterior part, of the nasopalatine duct. As in other Caimaninae, the secondary choanae occupy the posterior third of the anteroposterior length of the pterygoids and are bounded by them. Internally, the wide "heart-shaped" choanae are divided by a median bony septum formed by pterygoids. This bony septum projects anteriorly, occupying almost the entire posterior half of the palate. Posteriorly, the pterygoids project dorsally, reaching the lateral wall of the braincase and forming a suture with the laterosphenoid bridge, and in occipital view they contact the basisphenoid. The suture between pterygoids and basisphenoid is nearer to the medial opening of the Eustachian tubes than in *C. yacare*.

Ectopterygoid. As in other crocodiles, the ectopterygoid delimits the suborbital fenestra posterolaterally and contacts the maxilla anterolaterally, the jugal posterolaterally, the pterygoids medially, and the descending process of the postorbital posteromedially.

Articular bone. The articular bone forms the posterior margin of the internal mandibular fe-

nestra, most of the articular fossa, and the medially directed retroarticular process. This process is trapezoidal in outline, with its posteromedial surface rounded and its medial surface bearing a small notch anterior to the glenoid cavity. The mandibular foramen aërum is situated lateral to this notch (Figs. 3C and 4E,F) and displaced from the medial border of the retroarticular process. The dorsal surface of this process is slightly concave without the posterior protuberance present in *C. yacare*. The glenoid cavity is bounded posteriorly, anteriorly, and medially by the articular. It is subrectangular in shape, with the anterior and posterior margins concave and the medial and the lateral margins convex. The articular contacts the surangular laterally and the angular posteroventrally.

Angular bone. In lateral view, the angular contacts the surangular posterodorsally and the dent anterodorsally, forming most of the ventral margin of the external mandibular fenestra and part of the retroarticular process. In lateral view, the posterior border of the lower jaw forms an 120° angle, approximately, so the mandible is higher posteriorly. In lingual (medial) view, the angular contacts the splenial anteriorly, the coronoid anterodorsally, and the articular posterodorsally, forming part of the ventral margin of the internal mandibular fenestra and delimiting the foramen intermandibularis caudalis posteriorly (Fig. 3B).

Surangular bone. As in other caimans, the surangular bone projects posteriorly by means of a process that almost reaches the posterior border of the retroarticular process and forms the lateral margin of the glenoid cavity (Fig. 3A,C). In lateral view (Fig. 3A), the surangular bone contacts the dentary bone anteroventrally, and the angular posteroventrally, forming the posterodorsal margin of the external mandibular fenestra. The suture between surangular bone and dentary bone reaches the fenestra anterior to its posterodorsal corner, a general condition for alligatoroids (Brochu, 1999). Medially, the surangular contacts the splenial bone and the coronoid.

Dentary bone. As stated above, in *C. latirostris* the length of the symphysis shows intraspecific variation, extending to the level of the fifth, fifth–sixth alveoli (Fig. 3C). The number of mandibular teeth varies between 17 and 19. In lateral view, the dentary bone contacts the surangular bone dorsally and the angular bone ventrally. The dorsal margin of the dentary bone is wavy showing two stout flexures, one positioned anteriorly, from the first to fourth alveoli, and the second one posteriorly from the fifth to the tenth alveoli. These curvatures are also slightly developed in dorsal view (Fig. 3C). In lateral view, the dentary bone delimits the dorsal and anterior margins of the external mandibular fenestra, a condition different from that in *C. jacare*. Posteriorly, the dentary projects gradually in a dorsal direction and contacts the splenial bone in medial view.

Splenial bone. As in all Caimaninae, the splenial of alligatorids is excluded from the mandibular symphysis and projects dorsally to the Meckelian groove (Brochu, 1999: 43, figure 31; adapted from Clark, 1994: 66, 91, character 77). The splenial extends along the medial surface of the mandible forming the medial wall of the Meckelian canal. As in other caimanines, the splenial bears a small foramen intermandibularis oralis (Fig. 3B; see below) and contacts the coronoid posterodorsally and angular posteroventrally, delimiting together with the latter, the foramen intermandibularis caudalis. Laterally, it contacts the dentary bone, forming the medial border of the twelfth or thirteenth alveoli.

Coronoid. The coronoid is a ventrally elongated and crescent-shaped bone that delimits the Meckelian fossa anteriorly and anteroventrally. Together with a portion of the surangular bone, the posterodorsal surface of the coronoid serves as an attachment area for the transiliens cartilage (Fig. 3B). The coronoid contacts the splenial anteriorly and the angular ventrally. As in *Melanosuchus* Gray and other *Caiman* species, the foramen intermandibularis oralis medius is present in adult specimens of *C. latirostris*.

Cranial Musculature

Trigeminal muscles. These muscles comprise the adductor chamber, the main component of the cranial musculature that takes up most of the temporal fossae and the ventral sector of the orbit. This musculature is traversed by several cranial nerves and the muscular fibres are interdigitated, making it difficult to establish the limits of each muscle.

MAME. The MAME occupies the anterolateral portion of the infratemporal fossa. (Fig. 5A) It is attached to the ventral surface of the quadrate and quadratojugal bone, passes ventrolaterally to the jugal bar and inserts mainly on the dorsal margin of the surangular bone and transiliens cartilage (Schumacher, 1973), from the coronoid crest to the anterior sector of the glenoid cavity. Part of the attachment area on the ventral surface of the quadrate is formed by the quadrate aponeurosis (Iordansky, 2000), which is also attached to crests A and B (Iordansky, 1964) and vertically oriented. In *C. latirostris*, the MAME is divided into three superficial, medial, and deep main parts (Iordansky, 1964; Van Drongelen and Dullemeijer, 1982). Iordansky (2000) considered this muscle to be formed by two muscular packages in crocodiles, the *M. adductor mandibulae externus superficialis* (= superficialis + medialis *sensu* Iordansky, 1964 and Van Drongelen and Dullemeijer, 1982), and

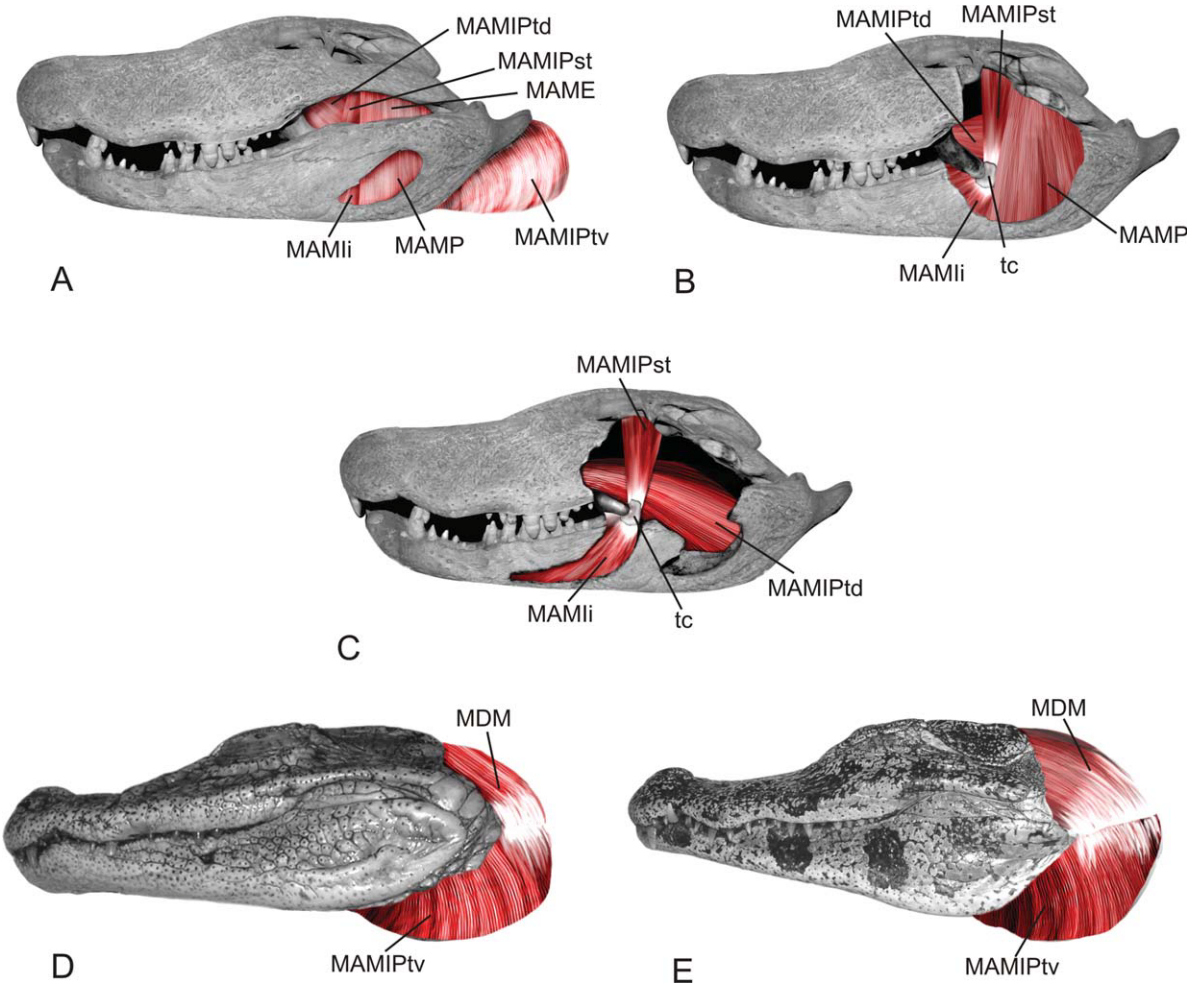

Fig. 5. Cranial muscles in *Caiman*. **A–C**, Lateral view of trigeminal muscles in *C. latirostris*; **D** and **E**, lateral view of *M. depressor mandibulae* and *M. pterygoideus ventralis*. D, *C. latirostris* and E, *C. yacare*. MAME, *M. adductor mandibulae externus*; MAMIi, *M. intramandibularis*; MAMP, *M. adductor mandibulae posterior*; MAMIPst, *M. pseudotemporalis*; MAMIPtd, *M. pterygoideus dorsalis*; MAMIPtv, *M. pterygoideus ventralis*; MDM, *M. depressor mandibulae*; tc, transiliens cartilage.

profundus. The deepest *pars* originates at the ventral margin of the parietal and squamosal bones, runs vertically and inserts into the coronar aponeurosis (see Iordanky, 2000; table 1) and posterodorsally to the transiliens cartilage. In lateral view, this *pars* is anterior to the medial *pars*. The latter is represented by a muscular mass situated dorsomedially to the superficial pars. Its fibers extend from the ventral surface of the quadrate lateral to crest A, running parallel and obliquely oriented in a dorsomedial–ventrolateral direction. In its posterior part, the separation between MAME and MAMP is not clear because their fibers are interdigitated. The medial *pars* attaches medially to the pars superficialis and anteriorly to the mandible by the coronar aponeurosis (see Iordansky, 2000; figure 1). In lateral view, the superficial *pars* is exposed as a muscular mass lateral to the medial *pars*; it is attached to the descending process of the quadratojugal–quadrate and contacts the postorbital (*sensu* Van Drongelen and Dullemeijer, 1982). Its fibers are dorsomedially–ventrolaterally oriented and insert mainly on the dorsal border of the surangular.

MAMP. Together with MAME, this muscle occupies the dorsal and posterior portion of the infratemporal fossa (Fig. 5A,B). Proximally the MAMP is positioned lateral to the V3 trigeminal nerve branch. This muscle originates on the ventral surface of the quadrate by the quadrate aponeurosis (*sensu* Iordanzky, 2000; "tendons A and B" of Iordansky, 1964 or "aponeuroses II and IV" *sensu* Van Drongelen and Dullemeijer, 1982: 347) and attaches to the medial border of the articular by means of the subarticular aponeurosis, to the medial margin of the angular by the angular aponeurosis, and to the medial area of the surangular and caudal portion of the transiliens cartilage, by the coronar aponeurosis (Iordansky, 2000; figure 1). The MAMP is also attached to the Meckel's cartilage and occupies the Meckelian fossa, covering the external mandibular fenestra; at this level it is

attached by an aponeurosis-like fibrous connective tissue. Its fibers are mostly ventrolaterally oriented but slightly slanted posteriorly.

MAMI. The *M. pseudotemporalis* is attached to the laterosphenoid. Its fibers run dorsoventrally and are placed medial to the V2 and anteriorly to the V3 trigeminal branches (Fig. 5A–C). The proximal portion of this muscle (near to the origin) is anteromedial to the deep *pars* and anterior to the medial *pars* of MAME and attached to the dorsal surface of the transiliens cartilage. As in other crocodiles, in *C. latirostris* we recognized two portions. The first is slender and anterolaterally positioned, attached to the laterodorsal surface of the laterosphenoid and inserted onto the dorsal surface of the transiliens cartilage. The second was deeper, positioned medial to the V3 branch of the trigeminal nerve, and attached to the laterosphenoid bridge and inserted on the coronar aponeurosis *sensu* Iordansky (2000). Holliday and Witmer (2007) identified these two *pars* as *M. pseudotemporalis superficialis* (which comprises the *M. intramandibularis*) and *M. pseudotemporalis profundus*.

M. intramandibularis. This muscle is attached to the fan-shaped intramandibular aponeurosis (Iordansky, 2000; figure 1) that projects anteroventrally into the Meckelian canal from the ventral surface of the transiliens cartilage (Fig. 5A–C). Its fan-shaped fibers are anteroventrally oriented and insert on the medial surface of the dentary bone, splenial bone, angular bone, and Meckelian cartilage. This cartilage is a hyaline longitudinal bar that extends along the ventral border of the mandible at the level of the mandibular symphysis. Holliday and Witmer (2007) considered *M. intramandibularis* as a mandibular portion of the *M. pseudotemporalis superficialis*.

M. pterygoideus dorsalis. This muscle is attached to the medial and anterior margin of the suborbital fenestra at the palatine and to the maxilla and prefrontal bones and the orbitonasal and interorbital cartilages (Fig. 5A–C). Its fibers run mainly in an anteroposterior direction, occupying the suborbital fossa and inserting anterolaterally and posteromedially to the mandibular tendon, dorsal to the deepest *pars* of MAMI *pseudotemporalis*.

M. pterygoideus ventralis. This muscle is situated in the ventral and posterior parts of the infratemporal fossa and the posterior and posteroventral parts of the mandible (Figs. 5A,B,D,E, and 6A). It attaches to the posteriodorsal surface of the pterygoid and the pterygoidal aponeurosis (*sensu* Iordansky, 2000). This aponeurosis is formed by three sheets, two vertical (lateral and medial) sheets connected by one horizontal (ventral) sheet. The ventral horizontal sheet is attached to the posterior margin of the pterygoid, the medial sheet is dorsally attached to a medial sheet of the quadrate aponeurosis and ventrally to the ventral sheet. The lateral sheet is anteriorly attached to the lateral margin of the pterygoid and the lateroposterior margin of the ectopterygoid and extends posteriorly and continuously to the ventral sheet. The fibers of the *M. pterygoideus ventralis* extend as several fan-shaped sheets and insert at the mandible by the angular and retroarticular aponeurosis onto the posterior and medial border of the retroarticular process.

M. intermandibularis. This muscle is attached to the anterior half of each splenial bone, occupying the anterior intermandibular space on the dorsal part of the medial surfaces of the splenial bone. Anteriorly, its fibers run transversally from hemimandible to hemimandible; posteriorly, the fibers insert in a medial raphe.

Facial muscles.

M. constrictor colli. This muscle is divided into two portions, one superficial and the other deep (Figs. 5D,E, 6A,B). The superficial portion is represented by a *pars oralis* and a *pars aboralis*. The *pars oralis* is attached to an aponeurosis of *M. pterygoideus ventralis*, and its fibers run transversally to the sagittal plane behind the *M. intermandibularis* and insert onto a medial tendinous raphe. The deep portion, *M. constrictor colli profundus* (= *M. interhyoideus* of Iordansky, 2000) attaches laterally to the first two cervical vertebrae (*sensu* Schumacher, 1973) and inserts on the posteroventral tendinous zone of the hyoids. Its horizontal fibers are perpendicular to the sagittal plane and surround the trachea.

MDM. In occipital view, the MDM is ventrally in contact with the superficial neck musculature (Fig. 5D). It attaches to the posterodorsal margin of the supraoccipital and squamosal and to the posterodorsal surface of the quadrate. The fibers of the MDM insert on the dorsal surface of the retroarticular process. In lateral view, it is rectangular shaped with the fibers obliquely oriented at an angle of approximately 45°.

Glossopharyngeal muscles

M. branchiomandibularis visceralis. This muscle is attached laterally to the hyoids via an aponeurosis lateral to the *M. hyoglossus*, in the insertion zone of the *M. hyoglossus* on the hyoids (Fig. 6A,B). The fibers of *M. branchiomandibularis visceralis* run anteriorly and slightly obliquely and insert on the anteroventral surface of the angular, covering in part the lingual foramen.

Hypoglossal muscles.

M. branchiomandibularis spinalis. This muscle is attached to the basal end of the *Cornu branchiale I* of the hyoid apparatus (Schumacher, 1973: 185; figure 54). In *C. latirostris*, the fibers of this muscle run parallel and insert anteriorly on the medial and dorsal surface of the splenial (Fig. 6A,B).

M. hyoglossus. In *C. latirostris*, this muscle is formed by a *pars medialis* and a *pars lateralis*. The latter *pars* is attached to the dorsolateral and

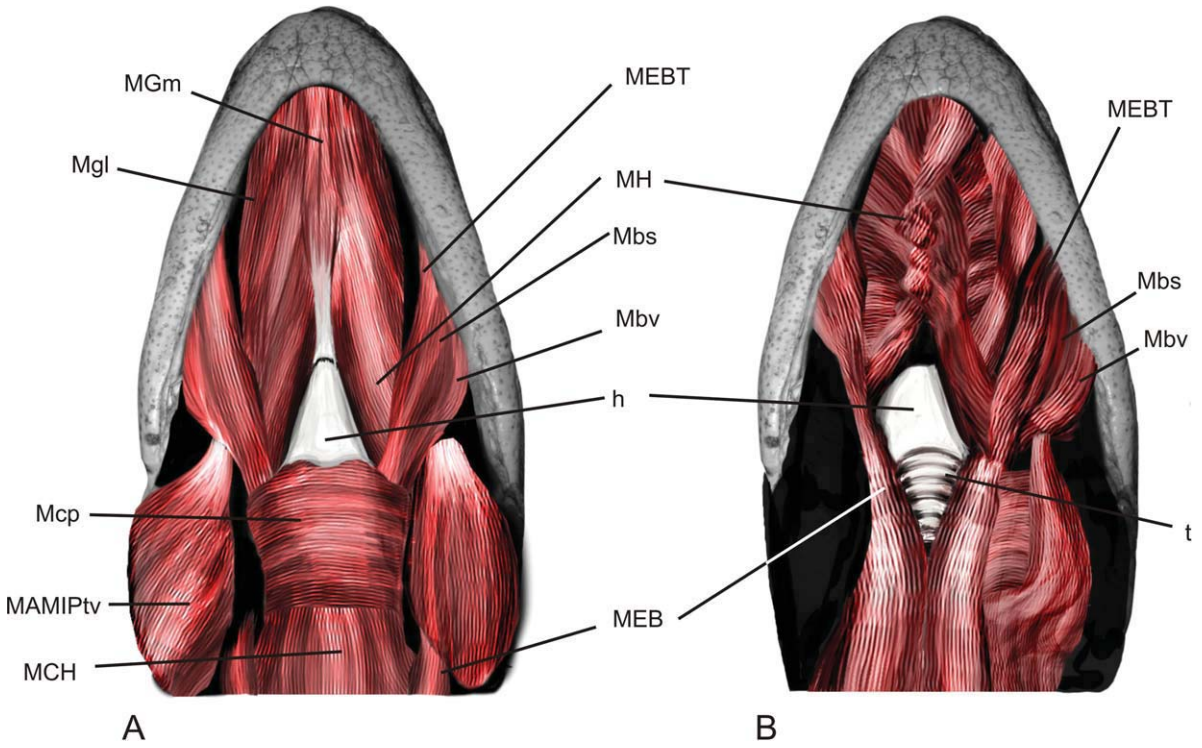

Fig. 6. Ventral view of cranial muscles in *C. latirostris*. **A**, superficial dissection; **B**, deeper dissection. h, hyoid; MAMIPtv, *M. pterygoideus ventralis*; Mbs, *M. branchiomandibularis spinalis*; Mbv, *M. branchiomandibularis visceralis*; MCH, *M. coracohyoideus*; MCp, *M. constrictor colli profundus*; MEB, *M. episternobranchiotendineus*; MEBT, *M. episternobranchiotendineus*; Mgl, *M. genioglossuslateralis*; Mgm, *M. genioglossus medialis*; MH, *M. hyoglossus*; t, trachea.

posterior parts of the posterior corner of the hyoid (considered as the *Cornu branchiale* II of other sauropsids; see Schumacher, 1973), surrounding it. Its short fibers insert on a connective raphe at the base of the tongue. The better developed *pars medialis* is attached to an aponeurosis on the ventral border of the posterior corner of the hyoid. Its fibers run obliquely (medially) and are anteriorly interdigitated forming the tongue (Fig. 6B).

M. genioglossus. This muscle is attached to the mandibular symphysis and, like *M. hyoglossus*, comprises both a *pars medialis* and a *pars lateralis*. The narrow *pars medialis* extends posteriorly toward the anterior border of the hyoid, where it inserts by means of a tendon. The *pars lateralis* extends posterolaterally and surrounds the *M. hyoglossus* (Fig. 6A,B).

Hypobranchial longitudinal muscles.

M. coracohyoideus. The fibers of this muscle are arranged in two longitudinal bundles lateral to the *M. episternobranchiotendineus* and *M. episternobranchialis*, at both sides of the trachea (Fig. 6A). The fibers of *M. coracohyoideus* are attached to the coracoid, extend alongside the trachea and insert mainly on the posterior process of the hyoid or *Cornu Branchial II* (Fig. 6A,B).

M. episternobranchiotendineus. This muscle is attached to the sternum and extends anteriorly to the medial surface and posterodorsal margin of the splenial bone. Its longitudinal fibers are positioned lateral to *M. episternobranchialis*, and together with the latter cover the ventral surface of the trachea. In its anterior sector the fibers of the *M. episternobranchiotendineus* are laterally oriented (Fig. 6A,B).

M. episternobranchialis. This muscle is attached to the sternum and extends anteriorly as two bundles of longitudinal fibers medial to the *M. episternobranchiotendineus*. *M. episternobranchialis* (Fig. 6A,B) inserts on the ventrolateral area of the hyoid body medially to the *cornu branchialis I*.

Skull Measurements

As a result of the allometric analysis, we obtained a high positive correlation between skull traits and the overall skull size (Table 3). In both *Caiman* species the snout length increases with positive allometry through ontogeny (Fig. 7A; Table 3). The elongation of the snout occurs in the same way in both species from small-sized to big-sized specimens, so both species are practically indistinguishable from each other by their snout relative length in each ontogenetic state. Contrary to *C. yacare*, in *C. latirostris*, the interorbital space increases isometrically while increasing the skull length, so the relative position of the orbits in the midline would be determined in young specimens

TABLE 3. Results of the regression analysis of skull variables measured in relation to total skull as independent variable

Species	Dependent variables	*b*	CI	log *a*	r^2	*P*	Allometry
C. yacare	Snout length	1.10	1.07–1.13	−0.45	0.99	<0.05	+
C. latirostris	Snout length	1.14	1.08–1.19	−0.55	0.99	<0.05	+
C. yacare	Anterior snout width	1	0.91–1.09	−0.53	0.96	<0.05	No
C. latirostris	Anterior snout width	1.16	1–1.32	−0.80	0.96	<0.05	+
C. yacare	Posterior snout width	1	0.95–1.06	−0.35	0.98	<0.05	No
C. latirostris	Posterior snout width	1.07	0.93–1.22	−0.41	0.96	<0.05	No
C. yacare	Interorbital width	1.18	1.04–1.32	−1.46	0.95	<0.05	+
C. latirostris	Interorbital width	1.08	0.94–1.22	−1.19	0.97	<0.05	No

and remains invariable in relation to the anterior–posterior growth of skull during ontogeny (Fig. 7B; Table 3). *C. latirostris* is the widest snouted *Caiman*. This condition in the posterior sector of the snout (anteorbital width) is probably established early in ontogeny and differs from that of *C. yacare* from the first ontogenetic states (Fig. 7C). Nevertheless while in *C. yacare* the anterior snout width increases isometrically with the skull length (probably establishing the final snout shape in young specimens), in *C latirostris* this growth shows positive allometry. This positive allometric relationship with the anterior snout width and the skull length could be determining a change of the snout shape during ontogeny and the final characteristic broad-snouted shape of this species would be establishing late in ontogeny (Fig. 7D). These hypotheses would be tested in future morphometric analysis in a bigger sample of specimens of these two *Caiman* species.

DISCUSSION

The focus of this study was the anatomical analysis of the cranial osteology and myology of *C. latirostris*. Compared with other extant caimans, *C. latirostris* shows morphological differences at skull level that are discussed below. Generally, the cranial morphology of *C. latirostris* is an overall triangular outline in dorsal view, with the lateral

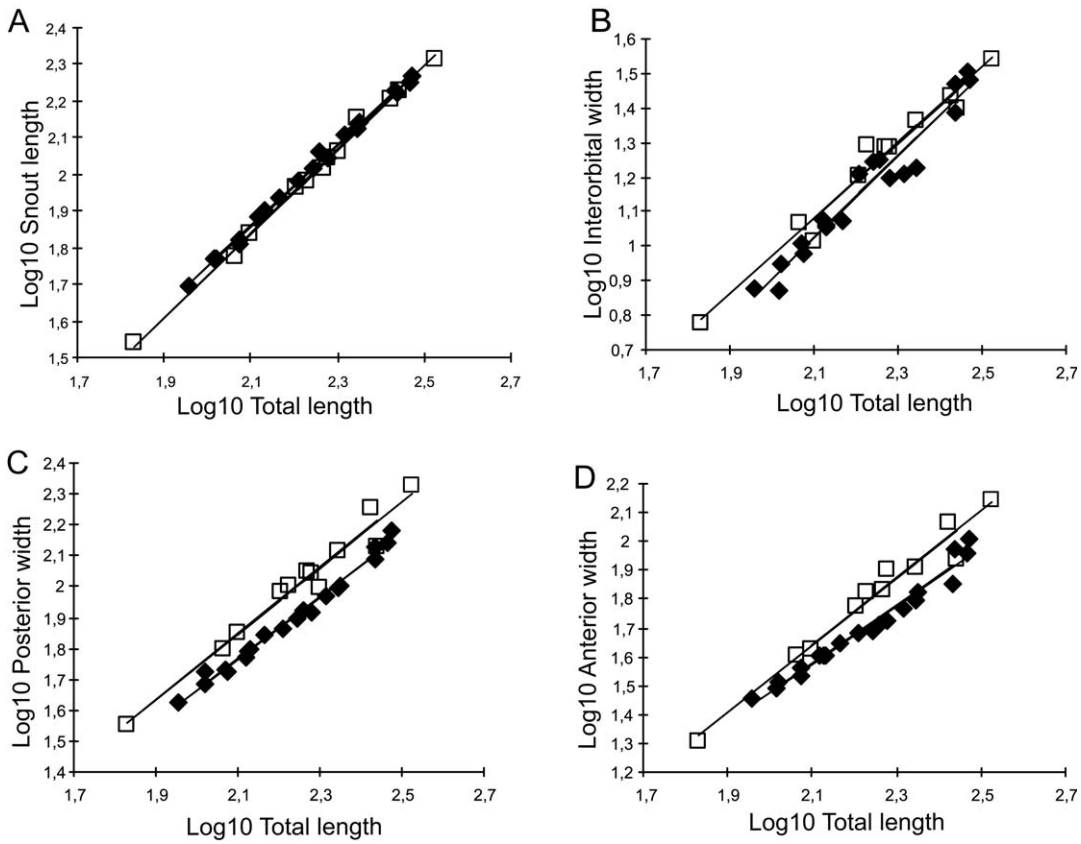

Fig. 7. Graphs of allometric equations calculated for different skull variables measured on 37 *Caiman* species differing in skull size. **A**, snout length; **B**, interorbital minimum width; **C**, posterior snout width; **D**, anterior snout width. The data are presented in logarithmic scale. Solid line: estimated allometric equation; white squares: *C. latirostris* specimens; black squares: *C. yacare* specimens.

margins converging in the snout region. Unlike the condition in *C. yacare* and *C. crocodylus*, the lateral curvature of the premaxilla–maxilla is slightly marked in lateral view and absent in dorsal view. The rostral crests of *C. latirostris* are well defined, and the medial flange of the orbits extends as a continuous crest on the prefrontal, the lacrimal, and the maxilla. This pattern is similar to the one in *Melanosuchus niger* (Spix), and the presence of very prominent rostral crests may be a shared character supporting the sister group relationship between *C. latirostris* and *M. niger* (Norell, 1988; Poe, 1997; Brochu, 1999). In *C. yacare* and *C. crocodylus*, the medial crest of the orbits is not prominent and extends anteriorly by a short crest through the prefrontal and lacrimal only. The occlusal pattern is the same in all alligatorids, with the dentary teeth occluding lingual to the maxillary toothrow. Nevertheless, some slight variation exists among the species of caimans, and in *C. latirostris* the first dentary teeth occlude posterior to the first tooth of the premaxilla such that never pierce the dorsal surface of this bone. In all specimens in which these teeth reach the upper jaw when the mouth is closed, the corresponding perforations are seen though the narial openings in the floor of the nasal cavity (Fig. 4C). In *C. yacare* and *C. crocodylus*, the first tooth occludes anteriorly, and when these teeth pierce the premaxilla, the perforations are anterior to the narial opening, on the dorsal surface of the bone (Fig. 4D). In many specimens of these species, the posterior surface of the first lower tooth perforates the anterior wall of the nasal cavity but never the floor of the latter. Another difference between *C. latirostris* and *C. yacare* is that the subtemporal fossa is less wider in *C. latirostris*, such that in occipital view the pterygoid–basisphenoid suture is near the basisphenoid–basioccipital suture. The higher position of the subtemporal fossa in *C. yacare* is related to the larger size of the *M. pterygoideus dorsalis* in this species. Similarly, and in contrast to *C. yacare*, in *C. latirostris* the lateral bridge of the laterosphenoid is complete in all studied specimens, and it is formed by a descending process of the laterosphenoid that is widely sutured to the pterygoid ventrally (Holliday and Witmer, 2009). Although the conformation and morphology of this bridge is variable in crocodiles (Brochu, 1999: 64; figure 52), in *Caiman*, this variation could be related to the anteroposterior extension of the ventral end of the laterosphenoid lateral process, which in *C. yacare* is narrow and not sutured to the pterygoid. By contrast, in *C. latirostris* the caudal bridge of the laterosphenoid is broadly sutured than the quadrate. The presence of this bridge is an ancestral condition of Alligatoridae that is present in all Caimaninae extant taxa. Posterolaterally to this bridge, on the ventral surface of the quadrate, two crests (A and B, Iordansky, 1964) correspond to the insertion of several portions of the adductor muscles (MAME and MAMP). Although these crests occur in all crocodiles, their relative size shows intraspecific variation in caimans. Anteriorly, crest A surrounds the posteroventral margin of the internal supratemporal fenestra. In *C. latirostris*, this crest is ventral to the foramen for the passage of the supraorbital nerve (sensu Holliday and Witmer, 2009) and probably the middle cerebral vein (Fig. 4A,B). In *C. yacare*, the relative position of this crest shows intraspecific variation, but it always located dorsal to or at the same level as this foramen, and never ventral to it as in *C. latirostris* (Fig. 4). Interspecific variation of mandibular bones was recorded in several structures of *Caiman*. In dorsal view, the glenoid cavity of *C. latirostris* possesses only a slight notch on the anterior margin (Fig. 3C), differing from the condition present in *C. yacare*, in which this anterior notch is pronounced, so that the glenoid cavity has a biconvex outline. In addition, the extension of the dentary bone along the ventral margin of the external mandibular fenestra also shows interspecific variation. In *C. latirostris*, the dentary bone is not extended as in *C. yacare*, forming a small anterior part of the ventral border of this fenestra, or even being excluded from this margin in some specimens.

Although the anatomy of jaw muscles of living crocodiles follow the same general "Bauplan" (Iordansky, 2000), and alligatorids seem to have a similar pattern of cranial musculature, this study revealed some differences with respect to previously published descriptions of caiman myology (Iordansky, 1964, 2000; Schumacher, 1973, 1985; Van Drongelen and Dullemeijer, 1982; Cleuren and De Vree, 1992, 2000; Holliday and Witmer, 2007). The anterior and posterior portions of the *pars profunda* of the MAME of *C. crocodylus* described by Van Drongelen and Dullemeijer (1982) was not observed in *C. latirostris*. Furthermore, in the latter species, this pars is attached to the parietal and squamosal, and not only to the parietal as in other crocodiles. In *C. crocodylus*, the superficial *pars* of MAME (*sensu* Iordansky, 2000) is attached to the quadrate (lateral to crest A), quadratojugal, and postorbital bones, but in *C. latirostris* this muscle did not reach the postorbital. The *M. pterygoideus dorsalis* in *C. latirostris* did not reach the pterygoid and lacrimal (Holliday and Witmer, 2007), and contrary to the case of *C. crocodilus* (Van Drongelen and Dullemeijer, 1982), the *M. pterygoideus ventralis* attaches to the posterodorsal surface of the pterygoid and the pterygoid aponeurosis, without contacting the dorsal and ventral surface of the pterygoid margin. In *C. latirostris*, the *M. intermandibularis* is attached to the anterior half of the splenial and posteriorly inserts by a medial raphe that serves as attachment zone for *M. constrictor colli*. An additional

difference observed in *C latirostris* and *C. yacare*, with respect to the available information published for other crocodiles (e.g., Iordansky, 2000), is that the *M. depressor mandibulae* attaches to the posterodorsal margin of the supraoccipital, squamosal, and the posterodorsal surface of quadrate. In lateral view in *C. latirostris*, this muscle is subrectangular and its fibers are obliquely oriented at an angle $<45^{\circ}$, differing from *C. yacare* in which this muscle is subtriangular and has oblique fibers oriented at an angle $\geq 45^{\circ}$ (Fig. 5D,E). The cranial musculature of *C. latirostris* also differs from that of other alligatorids in the following characteristics: 1) presence of a medial notch in the anterior margin of *M. constrictor colli profundus*; 2) the attachment area of *M. depressor mandibulae* does not include the parietals, as in Alligatorinae; and 3) the attachment area for *M. branchiomandibularis visceralis* is positioned more anteriorly than in *Alligator*.

These cranial muscles have been previously described mainly for *A. mississippiensis*, and the paucity of information about this musculature in caimans makes it difficult to analyze its morphological variability. The variability of cranial morphology in caimans needs to be reanalyzed within the phylogenetic context of the Caimaninae, first increasing the number of specimens and taxa and then analyzing the implications of this variation in a morphofunctional context. Furthermore, although the variation of cranial morphology observed here allows the recognition of potentially diagnostic (mainly osteological) characters, these hypotheses of homology should be phylogenetically tested to clarify their role in the evolutionary history of modern caimans.

As stated above, *C. latirostris* is the most extreme broad-snouted form among the *Caiman* species. This cranial shape is unique among extant Caimaninae (Fig. 1), and probably a reversal to the condition present in basal Globidonta alligatoroids (sensu Brochu, 1999). The rostral elongation of the skull of most of the extant Caimaninae species, not present in *C. latirostris*, increases the distance between the snout tip and the articular condyle. This general morphology could give a greater and faster movement for a given aperture angle of the mouth (Monteiro et al., 1997). This is probably an important feature related with the sideways movements of the head during underwater "fish catching." Furthermore, the major height of the subtemporal fossa in *C. yacare* is related to the larger size of the *M. pterygoideus* in this species, and could be related with an increased capacity to keep the prey in the mouth during feeding. The broad and short skull of *C. latirostris* could be advantageous for durophagy, a type of diet proposed for this species (Diefenbach, 1979, 1987). Monteiro et al. (1997) pointed out that an increase of the distance between the origin and insertion of the *M. depressor mandibulae* observed in posthatching *Caiman* specimens allows a greater extent of contraction and more control over the mandibular joint. However, the different angle of the fibers' orientation of the *M. depressor mandibulae* between *C latirostris* and *C. yacare* (Fig. 5D,E) could correspond to a lower force needed to open the mouth in *C. latirostris* and thus with less aquatic habits and type of diet for this species. *C. latirostris* is often found in slow-moving water in dense forest, although a wider variety of habitat types can be used when its range does not overlap with that of *C. yacare*. Nevertheless, these appreciations should be evaluated in a morphofunctional context, which is beyond the scope of the present analysis.

ACKNOWLEDGMENTS

The authors are grateful to the curators of the Herpetological Collections, JD Williams (Museo de La Plata) and J Faivovich (Museo Argentino de Ciencias Naturales "Bernardino Rivadavia") for allowing us to study the specimens under their care. Thank also to the staff of "El Cachape" (Chaco province) and "Proyecto Yacaré" (Santa Fe province) of Argentina who provided the *C. yacare* and *C. latirostris* specimens for dissections. The authors are grateful with R Battler and I Olivares for their comments and suggestions that improved this manuscript, M Tomeo and P Motta for the drawings and the design of the figures. This study was financed by the Agencia Nacional de Promoción Científica y Tecnológica, PICT N°473 directed by JB Desojo.

LITERATURE CITED

Brochu CA. 1999. Phylogenetics taxonomy, and historical biogeography of Alligatoroidea. J Vertebr Paleontol 19:9–100.

Brochu CA. 2003. Phylogenetic approaches toward crocodilian history. Annu Rev Earth Planet Sci 31:357–397.

Carvalho AL. 1951. Os jacarés do Brasil. Arqu Mus Nac 42:127–152.

Clark JM. 1994. Patterns of evolution in Mesozoic Crocodyliformes. In: Fraser NC, Sues HD, editors. In the Shadow of the Dinosaurs. New York: Cambridge University Press. pp 84–97.

Cleuren J, De Vree F. 1992. Kinematics of the jaw and hyolingual apparatus during feeding in *Caiman crocodilus*. J Morphol 212:141–154.

Cleuren J, De Vree F. 2000. Feefing in Crocodilians. In: Schwenk K, editor. Feeding. San Diego: Academic Press. pp 337–358.

Diefenbach COC. 1979. Ampullarid gastropod—staple food of *Caiman latirostris*? Copeia 1979:R162–163.

Diefenbach COC. 1987. Thermal and feeding relations of *Caiman latirostris* (Crocodylia: Reptilia). Comp Biochem Physiol 89:149–155.

Holliday CM, Witmer LM. 2007. Archosaur adductor chamber evolution: Integration of musculoskeletal and topological criteria in jaw muscle homology. J Morphol 268:457–484.

Holliday CM, Witmer LM. 2008. Cranial kinesis in dinosaurs: Intracranial joints, protractor muscles, and their significance for cranial evolution and function in diapsids. J Vertebr Paleontol 28:1073–1088.

Holliday CM, Witmer LM. 2009. The epipterygoid of crocodyliforms and its significance for the evolution of the orbitotemporal region of eusuchians. J Vertebr Paleontol 29:715–733

Iordansky NN. 1964. The jaw muscles of the crocodiles and some relating structures of the crocodilian skull. Anat Anz 115:256–280.

Iordansky NN. 1973. The skull of the Crocodilia. In: Gans C, Parsons TS, editors. Biology of the Reptilia, Vol. 4: Morphology D. New York: Academic Press. pp 201–262.

Iordansky NN. 2000. Jaw muscles of the crocodiles: Structure, synonymy, and some implications on homology and functions. Russ J Herpetol 7:41–50.

Legendre P, Legendre L. 1998. Numerical Ecology, 2nd ed. Amsterdam. Elsevier. 853 pp.

Monteiro LR, Cavalcanti MJ, Sommer HJS III. 1997. Comparative ontogenetic shape changes in the skull of *Caiman* species (Crocodylia, Alligatoridae). J Morphol 231:53–62.

Norell MA. 1988. Cladistic approaches and paleobiology as applied to the phylogeny of alligatorids. Ph.D. dissertation, Yale University, New Haven, Connecticut, 279 p.

Poe S. 1997. Data set incongruence and the phylogeny of crocodilians. Syst Biol 45:393–414.

Romer AS. 1956. Osteology of the Reptiles. Chicago: University of Chicago Press. 772 p.

Rowe T, Brochu CA, Colbert M, Merck JW Jr, Kishi K, Sglamer E, Warren S. 1999. Introduction to *Alligator*: Digital atlas of the skull. J Vertebr Paleontol 19:1–8.

Schumacher GH. 1973. The head muscles and hyolaryngeal skeleton of turtles and Crocodilians. In: Gans C, Parsons TS, editors. Biology of the Reptilia, Vol. 4. London: Academic Press. pp 101–199.

Schumacher GH. 1985. Comparative functional anatomy of jaw muscles in reptiles and mammals. Fortschr Zool 30:203–212.

Sedlmayr JC. 2002. Anatomy, evolution, and functional significance of cephalic vasculature in Archosauria. Ph.D. dissertation. Athens, Ohio: Ohio University, 398 p.

Van Drongelen Wv, Dullemeijer P. 1982. The feeding apparatus of *Caiman crocodilus*; a functional–morphological study. Anat Anz 151:337–366.

Walker AD. 1990. A revision of *Sphenosuchus acutus* Haughton, a crocodylomorph reptile from the Elliot Formation (late Triassic or early Jurassic) of South Africa. Philos Trans R Soc Lond B 330:1–120.

Witmer LM. 1995. The extant phylogenetic bracket and the importance of reconstructing solft tissues in fossils. In: Thomason JJ, editor. Functional Morphology in Vertebrate Paleontology. Cambridge, UK: Cambridge University Press. pp 19–33.